ELSEVIER

Biophysical Chemistry 93 (2001) 23–35

Biophysical Chemistry

www.elsevier.com/locate/bpc

Fluctuation of local points of F-actin sliding on the surface-fixed H-meromyosin molecules in the presence of ATP

Rieko Shimo, Koshin Mihashi*

Graduate School of Mathematics, Nagoya University, Furo-cho, Chikusa-ku, Nagoya, 464-8601, Japan

Received 3 April 2001; received in revised form 31 July 2001; accepted 3 August 2001

Abstract

F-actin fragments fluorescently labeled with rhodamine–phalloidin were copolymerized with non-labeled F-actin fragments. F-actin copolymer consisted of several bright (fluorescent) and dark (non-fluorescent) stripes of approximately 1 μm in width. Local motion of individual speckled F-actin was investigated by measuring translocation fluctuation of several tracing points marked on the actin filament. The tracing points included the borders between neighboring bright and dark stripes, as well as the tip and tail of the filament. For speckled F-actin with an average sliding speed of 4.6 μm/s at 23°C, the translocation distance of the tracing points (per 0.1 s) showed significant fluctuation, of the order of ±0.12 μm/s, approximately 25% of the sliding speed. The fluctuation correlation of the translocation distance between two tracing points decreased as the distance between them increased. Statistical analysis of the correlation length of the translocation distance L_c showed that L_c increased with the sliding speed of the actin filament. The sliding speed, however, saturated as the correlation length became close to the persistence length of the bending elasticity of F-actin. On the contrary, the correlation length of change in the translocation direction was essentially equal to the persistence length of F-actin, independent of the sliding speed. These results suggest that elasticity of the actin filament underlies the sliding velocity of F-actin.

Keywords: Fluctuation; Speckled F-actin; Fluctuation correlation; Correlation length of F-actin; Elasticity of F-actin

* Corresponding author. Tel.: +81-52-789-2833; fax: +81-52-789-2829.
E-mail address: mihashi@math.nagoya-u.ac.jp (K. Mihashi).

0301-4622/01/$ - see front matter
PII: S0301-4622(01)00203-4

1. Introduction

It has generally been understood that actin–myosin motility is elementarily based on the locomotion of the myosin–ATP head along F-actin. The energy for myosin locomotion is supplied by hydrolysis of ATP on the catalytic site of myosin. One of the crucial points of the motile process, which is still unsolved, is the temporal correlation between the motion of the myosin head and the catalytic process of ATP hydrolysis at the molecular level. In conventional muscle models, it is assumed that the internal work performed by myosin conformational changes that occur upon actin binding is localized to displacements of elastic elements associated with individual myosin heads [1,2]. It is also assumed in conventional muscle models that a myosin head rotation is coupled to a state-transition of the weak binding state of actin and myosin to their strong binding state [2,3].

Ishijima et al. [4] recently found that locomotion of a myosin head along a single F-actin is not directly coupled with a single catalytic step of myosin ATPase, but that it occurred intermittently in the course of hydrolysis of one ATP molecule. This suggested that the energy for mobility is first stored in myosin during catalytic reaction, then transferred to F-actin, followed by conversion into the mobile energy. According to Kitamura et al. [5], locomotion of the myosin head along the F-actin bundle occurred stepwise, and the unit size of the myosin steps was 5.3 nm, which was essentially equal to the distance between adjacent actin protomers along the homostrand of the F-actin helix. They also found that the average time interval between myosin steps was 3–5 ms, which was independent of the concentration of added ATP and became shorter with increased temperature. These facts suggested that the release of energy stored in the elasticity of the myosin head is a stochastic phenomenon.

Elastic energy released from myosin–ATP onto F-actin will cause extension of the elastic F-actin helix. Experimental evidence for this was given in an X-ray diffraction study of contracting muscle [6,7]. Compliance in actin and myosin filaments detected by these authors implies that myosin heads can freely exchange mechanical free energy with these filaments and with other myosin heads that interact with these filaments [8]. The additivity of free energy released from myosin to actin filaments found in fluorescence microscopy observations of sliding F-actin in an in vitro motility system [9,10] also suggested the importance of the filament elasticity of F-actin in the motile system. Elastic deformation associated with energy transfer between myosin and actin will probably occur at the interface of the two proteins, as well as in the F-actin helix. If this occurs as a stochastic phenomenon, fluctuation of the local structure of the F-actin helix may be significant and detectable, depending on the amount of elastic energy exchanged per unit time [10].

In the present study, we studied the fluctuation of locally marked points of F-actin which slid on the surface-fixed H-meromyosin–ATP. In order to detect fluctuation of local points of F-actin, speckled F-actin was used according to Hatori et al. [11]. The fluorescence stripes of speckled F-actin were obtained by copolymerization of two kinds of F-actin fragments, one labeled with rhodamine–phalloidin and the other with phalloidin only. Under a fluorescence microscope, the copolymer was marked with tracing points at the borders between adjacent, fluorescent bright and dark stripes. Motion of the borders was traced, as well as that of the tip and tail of F-actin. Since in an in vitro motility system, fluctuation of F-actin was biased by unidirectional sliding of the filament, we detected fluctuation of the local points of F-actin as the distance and direction of translocation of the multiple tracing points. We searched for relations between fluctuation parameters of the local points and the average sliding speed of F-actin.

2. Experiments and methods

2.1. Proteins

G-actin was extracted from acetone powder of rabbit skeletal muscle and purified according to Suzuki and Mihashi [12]. No special treatment

was carried out to exchange calcium ions bound to a specific site of G-actin with magnesium ions [13], and F-actin used in the present study contained 1 mol. of calcium ions in the specific site (Ca–F-actin). Myosin was prepared from rabbit skeletal muscle and purified according to Perry [14], and was frozen and stored at −80°C. H-meromyosin was obtained by α-chymotrypsin treatment of myosin [15]. H-meromyosin was used within 1 day after preparation.

2.2. In vitro motility assay system

2.2.1. Speckled F-actin (F-actin with fluorescent stripes)

Speckled F-actin with several fluorescent and non-fluorescent stripes was prepared in the following way, which was a slightly modified method of Honda et al. [10]. In F-buffer solution containing 100 mM KCl, 2 mM $MgCl_2$, 100 μM ATP and 10 mM Tris–HCl (pH 7.6), F-actin was fluorescence-labeled with an equal molar concentration of rhodamine–phalloidin (Molecular Probes, R-415). A 33-μg/ml solution of labeled F-actin was fragmented by sonication for 1–2 min. To this solution, G-actin (non-fluorescent) of a high concentration (1–5 mg/ml) was added to give an equal amount of labeled F-actin, and gently mixed. Phalloidin (non-fluorescent) was added to bring the total moles of phalloidin (phalloidin + rhodamine–phalloidin) to the same number of moles of actin. The solution was left standing for 15 min to promote polymerization of G-actin and copolymerization of fluorescent F-actin fragments. The solution was then left standing on ice for 3 h. F-actin thus obtained showed fluorescent stripes, mainly with a size of approximately 1 μm in width.

2.2.2. Flow-cell

Both cover slips and slide glasses were cleaned in KOH/ethanol by sonication according to [16], rinsed with distilled water (Milli-Q), and finally air-dried. Hydrophobic treatment of the cover slips was carried out with 0.1% nitrocellulose dissolved in isoamyl alcohol (a few drops), extra solution was removed and the slips were air-dried. On the surface of slide glasses, doubled spacer sheets of Teflon were fixed with vacuum paste. The volume of the flow cells obtained was 50 μl on average.

2.2.3. In vitro motility assay

The in vitro motility assay was carried out essentially according to the method of Kron and Spudich [16]. The solution for motility assay contained 25 mM KCl, 4 mM $MgCl_2$, imidazole–HCl 25 mM (pH 7.4), 0.05–2 mM ATP, 0.5% mercaptoethanol (solution AB) at 23°C. Fixation of H-meromyosin on the glass surface was carried out by introducing 40 μg/ml of H-meromyosin into a flow cell, which was placed upside-down to spread H-meromyosin uniformly on the glass surface. Excess solution was drawn by capillary action with a filter paper from one side of the flow cell. Another portion of 40 μg/ml H-meromyosin was introduced and the process described above was repeated. Free H-meromyosin in the flow cell was then washed out with 40 μl of AB solution 1 min later. The vacant space on the glass surface was coated with bovine serum albumin (BSA). Approximately 1 min after BSA coating, AB solution containing a few nanomoles of speckled F-actin was flushed into the cell. This was left standing for 30 s, then ATP (2 or 0.05 mM) and a portion of oxygen scavenger (final concentrations: 3.0 mg/ml glucose, 18 μg/ml catalase, 0. 1 mg/ml glucose oxidase) dissolved in AB solution was introduced. Extra F-actin was removed by this treatment.

2.3. Fluctuation analysis of fluorescence image of speckled F-actin

2.3.1. Fluorescence images

A Zeiss Axiovert 35 inverted fluorescence microscope was used for acquisition of the fluorescence images of F-actin. Installed in the microscope were a 100-W mercury lamp, 63× objective lens (Plan Apochromat, N.A. 1.4), and a filter set to select rhodamine fluorescence. Through an inter-tube (4×), fluorescence images were fed into a CCD camera after intensification with an ICCD unit (Hamamatsu Photonics, C2400-21). Output from the CCD camera was recorded on VHS tapes at 1/30 s video rate on a videotape

recorder (Panasonic, AG-DS550). Replaying the videotapes, fluorescence images were fed into an image analyzer at the rate of 1–2/30 s using the program HIMAWARI v. 1.6 (Library Co Ltd). The size of one pixel of the images obtained was 82 nm.

2.3.2. Tracing points on a speckled F-actin

On the fluorescence images of speckled actin filament, the borders between neighboring bright and dark stripes were marked as the tracing points of sliding F-actin. The coordinates of the tracing point were determined on the pixel where the intensity (brightness) gave half the value of the bright stripes of F-actin and the background level. The tip and the tail of F-actin were also included in the tracing points. These tracing points were called $P_1, P_2, \ldots, P_i$, starting from the tip of F-actin (Fig. 1). The coordinate of P_i at time t was denoted by $P_i(t)$. For fluctuation analysis, $P_i(t)$ were entered into the computer memory at 1/30-s intervals (video rate).

2.3.3. The translocation vector $V_i(t)$ of the tracing point P_i

Examination of the dynamic nature of a speckled actin filament sliding on H-meromyosin molecules was made by referring to the translocation vector $V_i(t)$ of P_i, which was defined as follows. A vector $V_i(t)$ which started from $P_i(t)$ and ended at $P_i(t+\Delta t)$ denoted the translocation of the tracing point P_i in a small time interval Δt.

2.3.4. The translocation distance $V_i(t)$ of the tracing point P_i

The size of the translocation vector $V'_i(t)$ was smoothed over the neighboring three terms by the moving average method, and noise was thus reduced:

$$V_i(t) \equiv \frac{1}{3} \cdot (V_i'(t-\Delta t) + V'_i(t) + V'_i(t+\Delta t)) \quad (1)$$

$V_i(t)$ thus obtained was the translocation distance of tracing point P_i. Possible error in the determination of $V_i(t)$ was ± 33 nm, which was estimated in following two ways. (1) The maximum reading error is one pixel, and according to the law of error transfer, the maximum error in $V_i(t)$ is 33 nm. (2) Taking the fluorescence image of a speck-

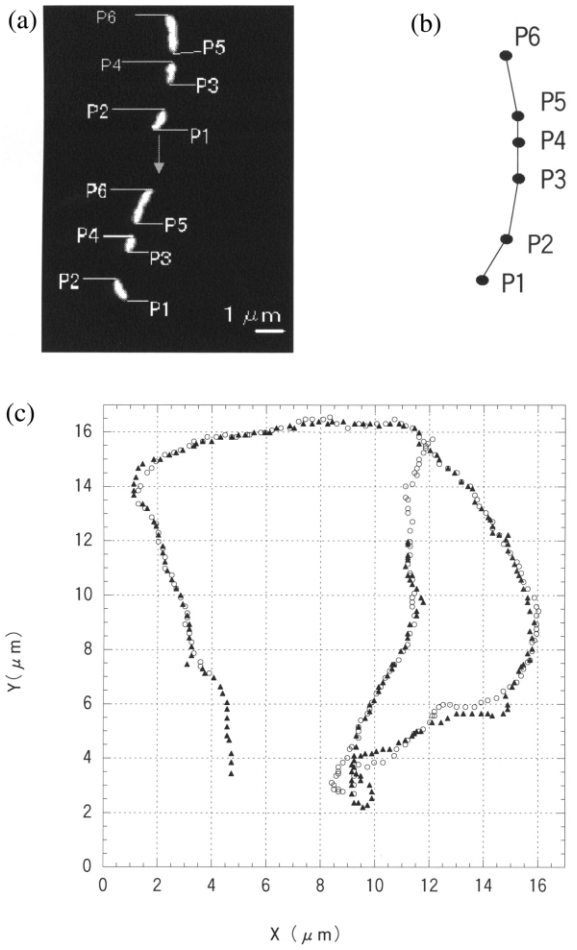

Fig. 1. (a) Superimposed picture of two photographs of a single, speckled F-actin filament sliding on the surface-fixed H-meromyosin taken at 1.8-s time interval. Six tracing points on the speckled F-actin (P_i; $i = 1$–6) which were used in the fluctuation analysis below are marked. (b) Image of a speckled F-actin in (a) is approximated with six tracing points P_i connected with straight lines. The distance between adjacent tracing points (i and j) is, according to Honda [10], called the skeleton length L_{ij} in the Madara approximation. (c) Trajectories of P_1 and P_5 of a single, speckled F-actin filament sliding on the surface-fixed H-meromyosin in the presence of 2 mM ATP at 23°C (a). The trajectories were drawn with the time series of positions of the tracing points at time intervals of 0.1 s. Trajectories started from the lower left part of the image.

led F-actin in its rigor state (in the absence of ATP), the maximum value of the spontaneous fluctuation of the tracing points was measured. The standard deviation of this spontaneous fluctuation ranged from 26 to 36 nm, and the average of 33 nm was adopted. Thus, two independent ways for estimation of the error gave the same value of 33 nm. We adopted this value as the experimental error in the translocation distance $V_i(t)$.

2.3.5. Translocation direction $Vd_i(t)$ of tracing point P_i

The direction of $V_i(t)$ was defined in terms of the angle θ between the translocation vector $V_i(t)$ and the abscissa (identical to the x-axis of the fluorescence images). After smoothing with the moving average method, we obtained the translocation direction $V\mathrm{d}_i(t)$ for individual tracing points. Fluctuation analysis was carried out on the rate of direction change calculated in the following equation.

$$\Delta V\mathrm{d}_i(t) \equiv \frac{(\theta_i(t+\Delta t) - \theta_i(t))}{\Delta t} \quad (2)$$

Fluctuation correlation was calculated using $\cos[\Delta V\mathrm{d}_i(t)]$ (a continuous function) instead of $\Delta V\mathrm{d}_i(t)$ itself in order to avoid changes in sign, which would not be appropriate for correlation analysis.

2.3.6. 'Skeleton length' of a speckled actin filament in 'Madara approximation'

The length between two neighboring tracing points of a speckled actin filament (P_i and P_j, $i<j$) was approximated by the distance (or the sum of distances) L_{ij} (Madara approximation [10]) which are given as follows. (1) If $j=i+1$, L_{ij} is the distance between P_i and P_{i+1}. (2) If $j \neq i+1$, $L_{ij} \equiv \sum_{i \le m < m+1 \le j} \mathrm{L}_{m,m+1}$ (skeleton length L_{ij} according to Honda [10]). The total length of a speckled F-actin was approximated by simply summing the distances $L_{i,i+1}$ between P_i and P_{i+1} from the tip to the tail of F-actin (Fig. 1) and was called the skeleton length L_{ij}.

3. Results

3.1. Selection of the time-scale in fluctuation analysis

In the present study, fluctuation of local motion of a single actin filament was characterized in terms of the translocation distance $V_i(t)$ of multiple tracing points P_i per 0.1 s. Selection of the time-scale of 0.1 s was important, since if it was too short, the translocation distance $V_i(t)$ was very short and its determination suffered seriously from the noise that is inevitable in image analysis. In this case, the translocation correlation measured between adjacent tracing points did not have any significant information (Fig. 2). On the other hand, if the time-scale for measuring the translocation was too long, the translocation distance became close to the average sliding speed of F-actin, and fluctuation correlation between neighboring tracing points approached the maximum (Fig. 2). On the basis of the results shown in Fig. 2, we judged that the 0.1-s time-scale was suitable for fluctuation measurement of the translocation distance of the tracing points of F-actin. Using the same reasoning when analyzing F-actin with a lower sliding speed, the time-scale was increased to maintain a constant signal/noise ratio (see Section 3.2).

Fig. 3a–c show a time series of the translocation distances $V_1(t)$, $V_2(t)$ and $V_6(t)$ of a speckled F-actin filament. $V_i(t)$ is given at every 1/30 s (video rate), one-third of the time scale used for measurement of the translocation distance V_i described above. Note that the importance of the time-scale selection for translocation determination just described above was independent of the time interval of 1/30 s of the time series of $V_i(t)$.

3.2. Cross-correlation of the translocation distance between two tracing points — propagation speed and the correlation length

3.2.1. Cross-correlation between pairs of tracing points

The cross-correlation of fluctuation between two tracing points P_i and P_j is defined as:

$$C_{ij}(\tau) \equiv \frac{\mathrm{COV.}\left(V_i(t), V_j(t+\tau)\right)}{\sigma_{V_i} \cdot \sigma_{V_j}} \quad (3)$$

where τ is the time shift between P_i and P_j and σ_{Vi}, is the standard deviation of $V_i(t)$. Prior to fluctuation analysis of a single actin filament, however, the value of $C_{ij}(0)$, where i,j belong to different speckled F-actins was examined, since we needed to know the critical value of the cross-correlation necessary to judge whether correlation between any two tracing points was significant (exceeding the noise level). We then analyzed 166 pairs of tracing points (randomly selected), each of which belonged to different speckled F-actins. Distribution of the cross-correlation $C_{ij}(0)$ of these 166 pairs ranged from -0.40 to 0.55. Of these 166 pairs, the cross-correlation of 90% (149 pairs) distributed in the range -0.3–0.3 and 72% (119 pairs) in the range -0.2–0.2. Therefore, we concluded that if $C_{ij}(\tau)$ is in the range -0.3–0.3, there is no correlation.

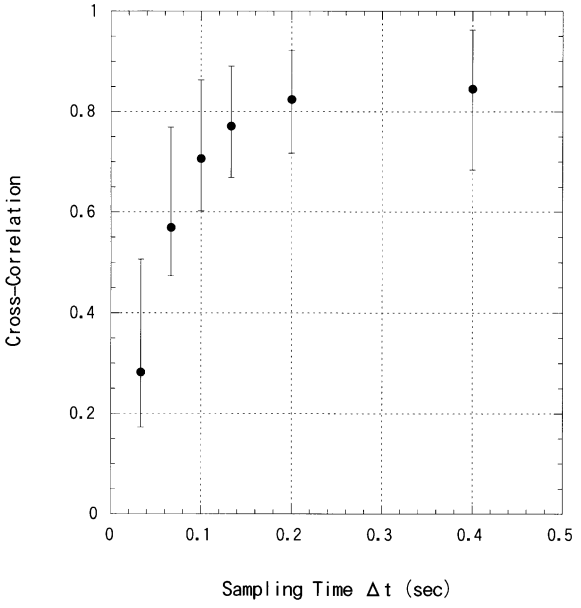

Fig. 2. Selection of sampling time-scale Δt most adequate for obtaining the translocation vector $V_i(t)$. Fluorescence images of a sliding speckled F-actin filament were stored in a computer memory at video rate (every 1/30 s), from which the translocation vectors were obtained as a function of time-scales changing from 1/30 to 12/30 s. On each sampling time-scale, cross-correlation of the translocation distances of P_i and P_j of all possible combinations of P_i and P_j ($_6C_2 = 15$ pairs) were calculated. The 15 cross-correlations thus obtained were averaged. The averaged cross-correlations are shown as a function of sampling time Δt. Judging from the relation between the averaged cross-correlation and Δt, we selected $\Delta t = 0.1$ s as the most adequate sampling time-scale for obtaining the translocation vector of individual tracing points $V_i(t)$. In the case of speckled F-actin with a lower sliding speed, a longer value of Δt was adopted in order to maintain the signal/noise ratio at a constant level. Error bars in this figure indicate the maximum and minimum of the cross-correlation.

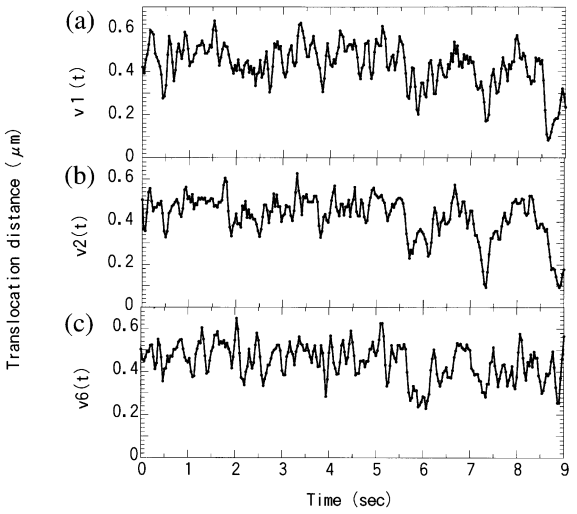

Fig. 3. Time sequence of the translocation distance (the size of the translocation vector) V_i (μm) per 0.1 s of the tracing points P_1, P_2 and P_6 of speckled F-actin shown in Fig. 1a (2 mM ATP, 23°C). In this figure, $V_i(t)$ at every 1/30 s are demonstrated: (a) $P_1(t)$, the tip point; (b) $P_2(t)$; and (c) $P_6(t)$, the tail point.

3.2.2. Propagation speed of the translocation distance fluctuation

The cross-correlation both between P_1 and P_2 and between P_1 and P_6 of a single speckled F-actin is shown in Fig. 4b. The following two points should be noted. Between P_1 and P_2 (which were 0.96 μm apart), the cross-correlation $C_{12}(\tau)$ was maximal at $\tau < 1/30$ s. Even between P_1 and P_6 (5.25 μm apart), the cross-correlation $C_{16}(\tau)$ was also maximal at $\tau < 1/30$ s. These results indicated that fluctuation propagated along this speckled actin filament at a speed faster than 5.25 μm/(1/30) s = 158 μm/s. The propagation speed

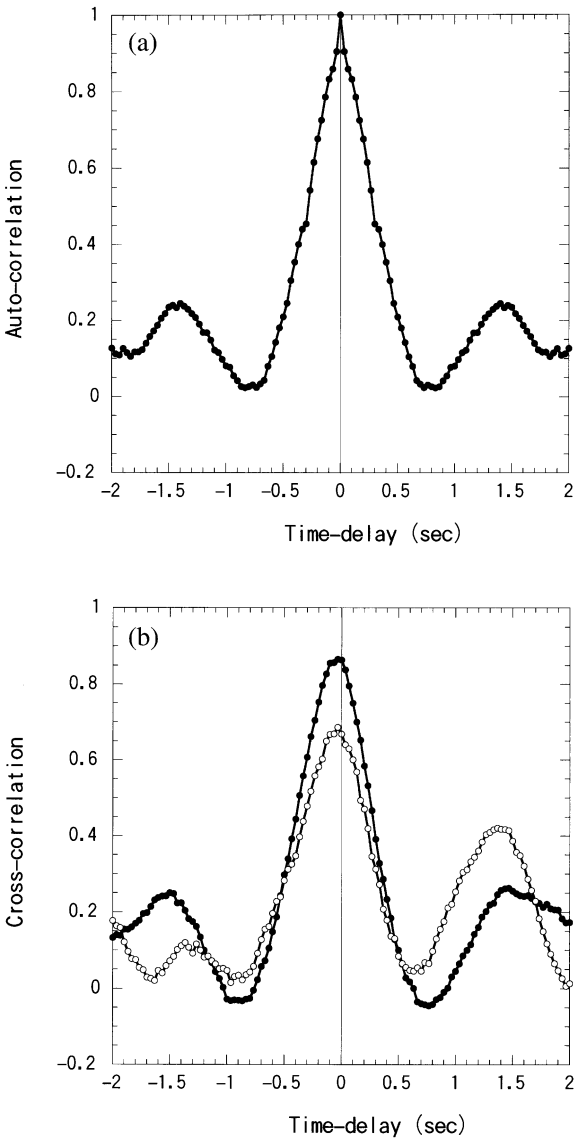

Fig. 4. Fluctuation correlation of the translocation distance $V_i(t)$ of a single speckled F-actin filament shown in Fig. 3. (a) Auto-correlation of $V_1(t)$. (b) Cross-correlation between $V_1(t)$ and $V_2(t)$ (●) and between $V_1(t)$ and $V_6(t)$ (○). Note that both of these cross-correlation had a maximum peak at time delay $\tau = 0$. This indicated that fluctuation propagated along F-actin at a speed at least equal to 5.25 μm/(1/30) s = 158 μm/s (where 5.25 μm was the skeleton length of this filament).

was more than 30-fold faster than the sliding speed of this actin filament. On the other hand, $C_{ij}(0)$ decreased depending on the skeleton length between i and j, i.e. $C_{12}(0) = 0.89$ and $C_{16}(0) = 0.69$ (Fig. 4b). [We use hereafter the notation $C_{ij}(0)$ in place of $C_{ij}(\tau = 0)$.]

3.2.3. Correlation length of the translocation distance fluctuation

The above results clearly show that fluctuation propagated along F-actin very much faster than the sliding of F-actin itself, but that the cross-correlation decayed during propagation along the actin filament. In order to demonstrate this point quantitatively, the correlation length of fluctuation L_c (of the translocation distance) was determined as follows. The cross-correlation values $C_{ij}(0)$ were calculated between all pairs of the tracing points (i,j) of a single, sliding F-actin filament and plotted as a function of the skeleton length L_{ij} between P_i and P_j. The results of two actin filaments with different sliding speeds (4.5 and 1.4 μm/s) are shown in Fig. 5. In both cases, $C_{ij}(0)$ decreased as L_{ij} increased, and the relation was approximated in the exponential form:

$$C_{ij}(0) \equiv \exp\left(-\frac{L_{ij}}{L_c}\right) \quad (4)$$

where L_c, the decrement of $C_{ij}(0)$, is an intensive quantity of F-actin (independent of its actual length). Apparently, L_c changed with the sliding speed of F-actin. The best fit of the data gave $L_c = 7.4$ and 1.8 μm for $V_s = 4.5$ and 1.4 μm/s, respectively. This result suggested that L_c and V_s may be interrelated. To confirm this point, statistical analysis with more than 10 F-actin filaments was carried out, and the results showed that an increase in V_s was in fact associated with an increase in L_c (Fig. 6). When the correlation length L_c approached the persistence length of the bending motion of F-actin (5–15 μm), which was determined previously [17,18], increase in the sliding speed tended to saturate (Fig. 6).

3.3. Fluctuation in the translocation direction of the tracing points

3.3.1. Cross-correlation of the translocation direction between tracing points

Correlation functions of fluctuation in the

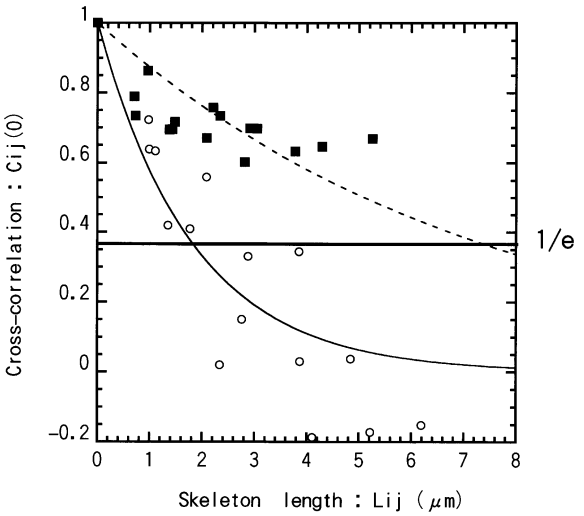

Fig. 5. The cross-correlation of sliding speckled F-actins in relation to their skeleton length L_{ij}. Of individual speckled F-actin, $C_{ij}(0)$, cross-correlation between the translocation distances V_i and V_j at $\tau = 0$ was calculated with respect to all pairs of P_i and P_j, and the $C_{ij}(0)$ values obtained were plotted as a function of the skeleton length L_{ij}. The exponential best fit of the data gave the correlation length L_c with respect to the translocation distance of each filament. (■) ATP 2 mM, $L_c = 7.2$ μm; (○) ATP 0.05 mM, $L_c = 1.8$ μm. We note that the total skeleton lengths of the above two F-actins were found at the longest skeleton lengths in this figure.

trans-location direction $\theta_i(t)$ of tracing points i were calculated using $\cos\theta_i(t)$ instead of $\theta_i(t)$ itself.

3.3.2. Propagation speed of the translocation direction fluctuation

Of all pairs of tracing points in a single F-actin, the maximum of cross-correlation in the translocation direction fluctuation appeared at a delay time (τM) which was proportional to the skeleton distance L_{ij}. This indicated that fluctuation of the translocation direction propagated backward along F-actin at a constant speed equal to L_{ij}/τM (Fig. 7). Two straight lines in Fig. 7 correspond to two single F-actins that moved with different sliding speeds. Interestingly, the propagation speed (slope in Fig. 7) was approximately equal to the sliding speed of each filament. In other words, the sliding speed of F-actin changed in association with the propagation speed of fluctuation of the translocation direction. This fact, in turn, indicated that a whole length of F-actin slid essentially on a single trajectory, which the leading part of F-actin had drawn on the surface-fixed H-meromyosin heads.

3.3.3. Correlation length in the translocation direction fluctuation

Cross-correlation of fluctuation in the translocation direction at $t = 0$ between all pairs of tracing points decayed with increasing skeleton length L_{ij} (Fig. 8). The decay rate did not significantly differ between two actin filaments shown in Fig. 7. In other words, the correlation length of fluctuation in the translocation direction did not depend on the sliding speed of F-actin, even though the propagation speed did. The correlation length of fluctuation in the translocation direction L_{dc} thus obtained was equal to 4.5 ± 0.2 μm/s, which was close to the persistence length of F-actin [17,18].

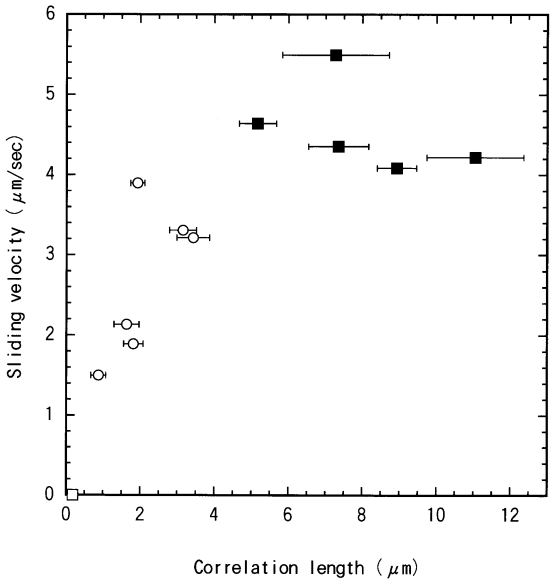

Fig. 6. The sliding speed of speckled F-actins (V_s) in relation to the correlation length with respect to the translocation distance (L_c) of the filament. Statistical analysis of 12 speckled F-actins showed that V_s increased with L_c, and the increase in V_s tended to saturate when L_c approached the persistence length of the bending motion of F-actin previously determined [17,18]. Solution conditions: (○) ATP 0.05 mM; (■) ATP 2 mM; and (□) without ATP (rigor condition).

This apparent coincidence may be quite reasonable, because the translocation direction of a tracing point is equal to the tangent at that point of F-actin, independent of its sliding speed. The correlation length of the translocation direction consequently corresponds to the persistence length of F-actin, although the former is under the influence of myosin–ATP interaction, with the latter being defined in equilibrium condition (Table 2). These results may suggest that the translocation direction or curvature of sliding F-actin is principally determined by the elasticity of F-actin rather than by the influence of myosin–ATP.

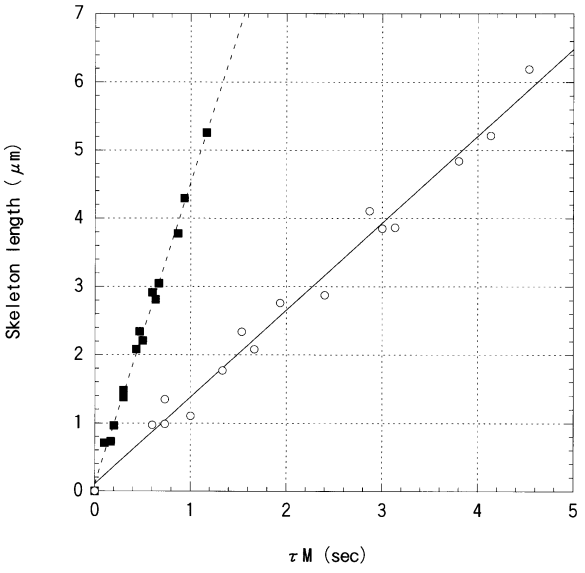

Fig. 7. Propagation of fluctuation in the translocation direction. The rate of direction change of the vector $\langle \boldsymbol{V_i(t)} \rangle$ was calculated according to the equation $\Delta V\mathrm{d}_i(t) = [\theta_i(t+\Delta t) - \theta_i(t)]/\Delta t$, where θ is the angle between the translocation vector $\langle \boldsymbol{V_i(t)} \rangle$ and the abscissa (identical to the x-axis of the fluorescence images). Cross-correlation between $\Delta V\mathrm{d}_i(t)$ and $\Delta V\mathrm{d}_j(t+\tau)$, which corresponded to the skeleton length L_{ij}, was calculated using $\cos[\Delta V\mathrm{d}_i(t)]$ (a continuous function) instead of $\Delta V\mathrm{d}_i(t)$. The cross-correlation thus obtained gave a maximum peak at the delay time τ, and a linear relation between τM and L_{ij} was obtained, which depended on the concentration of ATP, as shown in the figure. The presence of these straight lines was evidence that the maximum cross-correlation moved backward on the speckled F-actin at a constant speed. Linear regression gave a slope of 1.4 (○, 0.05 mM ATP) and 4.5 μm/s (■, 2 mM ATP). Strikingly, the propagation rate of the maximum cross-correlation just coincided with the sliding velocity of the filament itself under the experimental conditions. This meant that a speckled F-actin slid in such a way that the trajectories of P_i ($i > 1$) essentially coincided with that of P_1.

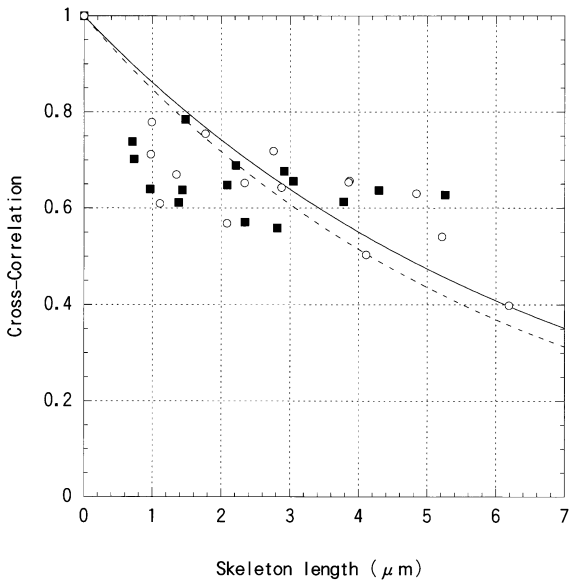

Fig. 8. Cross-correlation of the rate of direction change of the vector $V_i(t)$ between that of $V_j(t)$ in relation to the skeleton length L_{ij}. Using exponential best fits of the data, we obtained a correlation length L_{dc} equal to 6.7 ± 0.72 (○, 0.05mM ATP) and 5.70 ± 0.70 μm (■, 2 mM ATP), both of which were of the same order of magnitude of the persistence length of the bending mode of F-actin previously determined [17,18].

3.4. Non-uniformity of fluctuation along F-actin

In Table 1, fluctuation parameters of a particular single F-actin with six tracing points are given. The averaged translocation distance $V_i(t)$ per 0.1 s of these six tracing points was approximately 0.4 μm, indicating fluctuation of local points was almost constant along the actin filament, as previously reported [11]. It is also evident that fluctuation values for the translocation distance of each tracing point were almost of the same order of magnitude as each other. However, as shown in Table 1, the % fluctuation [i.e. the ratio of fluctuation to the averaged $V_i(t)$] was significantly larger in the anterior part of F-actin (at P_1 and P_2) than in other parts. We then proceeded with

Table 1
Characterization of six tracing points of F-actin

	Tracing points					
	P_1	P_2	P_3	P_4	P_5	P_6
Skeleton length, $L_{i-1,i}$ (μm)	–	0.96	1.24	0.86	0.67	1.44
Time average of $V_i(t)$, $[V_i]$ (μm)	0.42	0.41	0.43	0.43	0.43	0.43
Standard deviation of $V_i(t)$, σ_{Vi} (μm)	0.09	0.09	0.07	0.07	0.07	0.07
$\sigma_{Vi}/[V_i]$ ratio (%)	21	22	16	16	16	15

fluctuation analysis to determine if there was any non-uniformity of fluctuation among the tracing points located along a single F-actin filament. The translocation distance at time t averaged over six tracing points of the F actin,

$$\langle V(t)\rangle \equiv \frac{1}{6}\cdot\sum_{i=1}^{6} V_i(t) \tag{5}$$

showed a repetition of gradual increases followed by abrupt, deep decreases, just like a saw-tooth series of irregular sizes. Subtraction of this value of $\langle V(t)\rangle$ from each $V_i(t)$ of individual tracing points gave a time series of the excess fluctuation $[\Delta V_i(t)]$ for each tracing point. The excess fluctuation $\delta_i = \Delta V_i(t)$ at the tracing points P_1, P_3 and P_6 are shown in the form of a histogram in Fig. 9a–c. Of the tip point P_1, the histogram of the excess fluctuation δ_1 is apparently asymmetrical with a long minus-tail (Fig. 9a). Such tailing was absent in the histogram of P_3 and P_6. The minus-tailing in the histogram of δ_1 indicated that translocation of the tip point of F-actin showed a frequent and abrupt large decrease in speed. This was most significantly responsible for the saw-tooth phenomenon observed in $\langle V(t)\rangle$. We confirmed this anomaly in δ_1 by calculating the skewness (S_i) of the excess fluctuation δ_i of each tracing point i, defined as follows:

$$S_i \equiv \frac{1}{T}\cdot\sum_{t=1}^{T}\delta_i(t)^3 \Big/ \left(\sqrt{\frac{1}{T}\cdot\sum_{t=1}^{T}\delta_i(t)^2}\right)^3 \tag{6}$$

Here the skewness was defined with respect to the amount of excess fluctuation over $\langle V(t)\rangle$. The skewness (S_i) of each tracing point (Fig. 10a) indicated that the translocation speed of the anterior part (approx. 1 μm in length) of F-actin often drops deeply and abruptly, with such drops in sliding speed tending to disappear at the tracing points distant from the tip point. This phenomenon of an abrupt speed-down was found in almost all actin filaments studied, independent of the sliding speed of F-actin (Fig. 10b).

4. Discussion

4.1. Elasticity of F-actin in relation to sliding motility

On the surface-fixed myosin heads in the presence of a sufficient amount of ATP, F-actin slides with a constant speed, indicating that actin–myosin–ATP interaction is under steady-state conditions [18–21]. An unsolved question about the sliding motion of F-actin is the independence of the sliding speed of F-actin from its length. Since the F-actin length is proportional to the number of myosins interacting with it, observations reveal that the sliding speed of F-actin is primarily determined by the density of myosin along F-actin, or the average distance between adjacent myosins along F-actin. Actually, a decrease in the distance between adjacent myosins (i.e. increase in myosin density) resulted in an increase in the driving activity of myosin [21,22]. This suggested that some kind of cooperation between neighboring myosins may work to drive F-actin. On the other hand, Huxley [1] has proposed an intelligent model of the sliding mechanism of actin–myosin–ATP, in which individual myosin–ATP complexes work independently to drive F-actin. In the Huxley model, driving forces

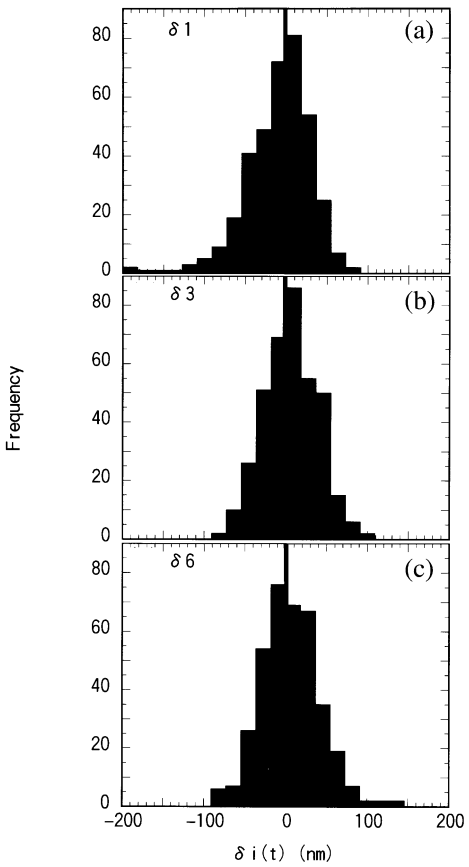

Fig. 9. Histograms of the excess fluctuation in the translocation speed of the tracing points of a speckled F-actin filament shown in Fig. 1. The excess fluctuation of the tracing point P_i at time t is given as $\delta_i(t) = V_i(t) - V(t)$, where $V(t)$ is the average of six $V_i(t)$ at time t. (a) δ_1 of the tracing point P_1 (the tip of filament); (b) δ_3 of the tracing point P_3; and (c) δ_6 of the tracing point P_6.

of individual myosins are additive, since F-actin is assumed to be a rigid, thin rod. As a consequence, the steady-state sliding speed of F-actin is explained in terms of the force balance principle between the total driving force and resistance, both of which are proportional to the length of F-actin. Huxley and Simmons extended the original force-balance model to explain transient phases of the change in tension in striated muscle after a sudden alteration of the muscle length [23]. In this advanced model, the elastic elements responsible for force generation in muscle are still confined within cross-bridges [23].

In the present study, we carried out fluctuation analysis of the translocation velocity of multiple tracing points marked on a single F-actin filament, which is driven by a large number of surface-fixed myosin–ATP complexes. Results showed that (1) the fluctuation propagated along the actin filament at least 30-fold faster than its sliding speed. However, it was also found that (2) the fluctuation of these tracing points of F-actin were significantly correlated, and the correlation length obtained was not infinitely long, which might be expected if F-actin really assumed the form of a rigid, thin rod. Thus, we may emphasize the importance of the elasticity of F-actin in the sliding motility of the actin–myosin–ATP system. We characterized the elasticity of sliding F-actin with several fluctuation parameters, as shown in Table 2. The only fluctuation parameter for which the correlation length changed in association with the sliding velocity of F-actin was the translocation distance. The correlation length of all other fluctuation parameters was independent of the sliding velocity. The latter parameters were of the same order of magnitude as the persistence length of the thermal bending motion of F-actin, which was under thermal equilibrium conditions (without interaction with myosin). These facts may suggest that the translocation direction Vd_i and the curvature φ_i of sliding F-actin are primarily determined by the bending elasticity intrinsic to F-actin, rather than by its interaction with myosin–ATP.

4.2. Possible deformation of local structure of F-actin helix where the elastic energy is transferred from myosin–ATP

What kind of structural change occurred in F-actin when the fluctuation correlation length L_c increased? Although a direct answer to this question has not yet been given by the present study, the following suggestions may be made. One of the most important features of the local fluctuation of F-actin shown in Fig. 3 was that the time-scale of changes in the translocation speed was at least one order of magnitude larger than the elementary duration of myosin–ATP–actin

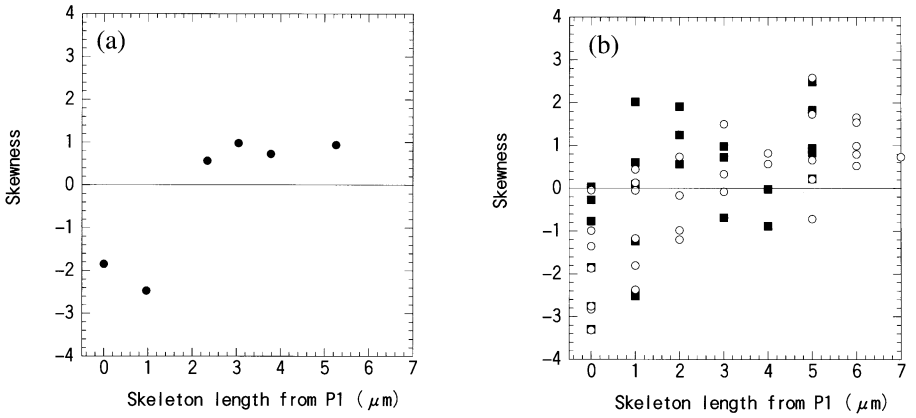

Fig. 10. Skewness (S_i) of the translocation speed of the individual tracing points of a speckled F-actin filament shown in Fig. 1 as a function of the skeleton length from P_1 to P_i (a) in the presence of ATP 2 mM. (b) Statistical analysis of the skewness of various lengths of F-actin in two concentrations of ATP: ○, 0.05mM; and ■, 2 mM ATP. In (b), data on skeleton length (from P_1) were grouped every 1 μm.

Table 2
Propagation speed and correlation length of fluctuations (at 23°C) in relation to the sliding speed (V_s) of F-actin

Sliding speed, V_s (μm/s)	Propagation speed (μm/s)		Correlation length (μm)	
	4.5	1.4	4.5	1.4
Translocation distance	> 158	> 158	7.4	1.8
$\Delta V\mathrm{d}_i$[a]	$\sim V_s$	$\sim V_s$	5.7	6.7
Curvature φ_i[b]	$\sim V_s$	$\sim V_s$	9.1	10.3

[a]$\Delta V\mathrm{d}_i$ was defined as follows. The angle α_i between the x-axis and the translocation direction $\boldsymbol{V_i(t)}$ was given after smoothing over the neighboring three angles formed between the x-axis and $\boldsymbol{V_i(t-\Delta t)}$, $\boldsymbol{V_i(t)}$ and $\boldsymbol{V_i(t+\Delta t)}$ by floating averages. From this value of the angle α_i, we calculated $\Delta V\mathrm{d}_i(t) \equiv \alpha_i(t+\Delta t) - \alpha_i(t)$.

[b]Curvature φ_i was defined as follows. We have a vector $\boldsymbol{R_{i,i+1}}$ which joins P_i and P_{i+1}. The angle between the x-axis and $\boldsymbol{R_{i,i+1}}$ is denoted as $\theta_{i,i+1}$. We then define the angle φ_i as $\varphi_1 \equiv \theta_{1,2} - \theta_{2,3}$, and so on.

interactions detected by Kitamura et al. [5]. It may therefore be suggested that the elementary forces exerted from a large number of myosin–ATP complexes were assembled to produce elastic deformation of a relatively large-scale structure of F-actin. In the helical structure of F-actin, elastic deformation may involve bending and twisting, as well as compression and elongation. Elastic energy transferred from myosin to the local structure of the F-actin helix may propagate along F-actin. Accumulation and dissipation of elastic energy may occur. The reasonably stochastic nature of these dynamic changes in the helical structure of F-actin may underlie the fluctuation of multiple tracing points observed in the present study.

References

[1] A.F. Huxley, Muscle structure and theories of contraction, Prog. Biophys. Biophys. Chem. 7 (1957) 255–318.
[2] T.L. Hill, Theoretical formalism for the sliding filament model of contraction of striated muscle. Part 1, Prog. Biophys. Mol. Biol. 28 (1974) 267–340.
[3] H.E. Huxley, The mechanism of muscular contraction, Science 164 (1969) 1356–1366.
[4] A. Ishijima, H. Kojima, T. Funatsu et al., Simultaneous observation of individual ATPase and mechanical events by a single myosin molecule during interaction with actin, Cell 92 (1998) 161–171.

[5] K. Kitamura, M. Tokunaga, A.H. Iwane, T. Yanagida, A single myosin head moves along an actin filament with regular steps of 5.3 nanometers, Nature 397 (1999) 129–134.
[6] H.E. Huxley, A. Stewart, H. Sosa, T. Irving, X-Ray diffraction measurements of the extensibility of actin and myosin filaments in contracting muscle, Biophys. J. 67 (1994) 2411–2421.
[7] K. Wakabayashi, Y. Sugimoto, H. Tanaka, Y. Ueno, Y. Takezawa, Y. Amemiya, X-Ray diffraction evidence for the extensibility of actin and myosin filaments during muscle contraction, Biophys. J. 67 (1994) 2422–2435.
[8] J.E. Baker, L.E.W. LaConte, I. Brust-Mascher, D.D. Thomas, Mechanochemical coupling in spin-labeled, active, isometric muscle, Biophys. J. 77 (1999) 2657–2664.
[9] T. Oda, Y. Shikata, K. Mihashi, Mutual sensitization of ATP and GTP in driving F-actin on the surface-fixed H-meromyosin, Biophys. Chem. 61 (1996) 63–72.
[10] H. Honda, K. Hatori, Y. Igarashi, K. Shimada, K. Matsuno, Contractile and protractile coordination within an actin filament sliding on myosin molecules, Biophys. Chem. 80 (1999) 139–143.
[11] K. Hatori, H. Honda, K. Shimada, K. Matsuno, Propagation of a single coordinating force generation along an actin filament in actomyosin complexes, Biophys. Chem. 75 (1998) 81–85.
[12] N. Suzuki, K. Mihashi, Subunit flow in F-actin under steady-state conditions. Application of a novel method to determination of the rate of subunit exchange of F-actin at the terminals, Biophys. Chem. 33 (1989) 177–193.
[13] K. Mihashi, M. Nakabayashi, H. Yoshinwra, H. Ohnuma, Absorption, fluorescence, and linear dichroism spectra of fluorescein mercuric acetate bound to F-actin, J. Biochem. 85 (1979) 359–366.
[14] S.V. Perry, Myosin adenosinetriphoshatase. $ATP + H_2O \rightarrow ADP + H_2PO_4$, Methods Enzymol. 2 (1955) 582–588.
[15] Y. Okamoto, T. Sekine, A streamlined method of subfragment one preparation from myosin, J. Biochem. 98 (1985) 1143–1145.
[16] S.J. Kron, J.A. Spudich, Fluorescent actin filaments move on myosin fixed to a glass surface, Proc. Natl. Acad. Sci. USA 83 (1986) 6272–6276.
[17] H. Nagashima, S. Asakura, Dark-field light microscopic study of the flexibility of F-actin complexes, J. Mol. Biol. 136 (1980) 169–182.
[18] F. Gittes, B. Mickey, J. Nettleton, J. Howard, Flexural rigidity of microtubules and actin filaments measured from thermal fluctuations in shape, J. Cell Biol. 120 (1993) 923–934.
[19] Y. Harada, K. Sakurada, T. Aoki, D. Thomas, T. Yandagida, Mechanochemical coupling in actomyosin energy transduction studied by in vitro movement assay, J. Mol. Biol. 216 (1990) 49–68.
[20] S.J. Kron, Y.Y. Toyoshima, T.Q.P. Uyeda, J.A. Spudich, Assays for actin sliding movement over myosin-coated surfaces, Methods Enzymol. 196 (1991) 399–416.
[21] T.Q.P. Uyeda, S.J. Cron, J.A. Spudich, Myosin step size. Estimation from slow sliding movement of actin over low density of heavy meromyosin, J. Mol. Biol. 214 (1990) 699–710.
[22] J.A. Spudich, S.J. Kron, M.R Sheetz, Movement of myosin-coated beads on oriented filaments reconstituted from purified actin, Nature 315 (1985) 584–586.
[23] A.F. Huxley, R.M. Simmons, Proposed mechanism of force generation in striated muscle, Nature 233 (1971) 533–538.